

# Strand Critical Current Degradation in Nb<sub>3</sub>Sn Rutherford Cables

Emanuela Barzi, Michela Fratini, Hugh C. Higley, Ron M. Scanlan,  
Ryuji Yamada, and Alexander V. Zlobin

**Abstract**—Fermilab is developing 11 T superconducting accelerator magnets based on Nb<sub>3</sub>Sn superconductor. Multifilamentary Nb<sub>3</sub>Sn strands produced using the Modified Jelly Roll, Internal Tin, and Powder-in-Tube technologies were used for the development and test of the prototype cable. To optimize the cable geometry with respect to I<sub>c</sub>, short samples of Rutherford cable with packing factors in the 85 to 95% range were fabricated and studied. The results of I<sub>c</sub> measurements made on the round virgin strands were compared with those made on the strands extracted from the cable samples. This paper addresses I<sub>c</sub> degradation issues related to cabling.

**Index Terms**—Critical current degradation, Nb<sub>3</sub>Sn strand, Rutherford cable, superconducting magnet.

## I. INTRODUCTION

WITHIN the framework of an R&D program towards a post-LHC Very Large Hadron Collider (VLHC), high field Nb<sub>3</sub>Sn dipole magnets (HFM) with a nominal field of 10-12 T are being developed at Fermilab. The first models feature 1 meter long two-layer shell-type (cos-theta) coils that use a keystone Rutherford-type cable made of 28 Nb<sub>3</sub>Sn strands 1 mm in diameter [1]. In such a design, the critical current density in the non-Cu section of the strand, J<sub>c</sub>, at 4.2 K and 12 T that is needed to reach a maximum field of 11 T is about 2000 A/mm<sup>2</sup>. However, the critical current, I<sub>c</sub>, of the original virgin strand can be reduced during magnet fabrication. Among the factors that reduce strand critical current are strand plastic deformation during cabling (before reaction), and cable compression in the coil (after reaction) during magnet fabrication and operation. This latter factor is due to J<sub>c</sub> sensitivity of Nb<sub>3</sub>Sn to strain [2].

This paper addresses I<sub>c</sub> degradation issues related to strand I<sub>c</sub> degradation during cabling.

## II. STRAND AND CABLE DESCRIPTION

### A. Strand and Cable Parameters

Several kilometers of multifilamentary Nb<sub>3</sub>Sn strands produced using the Modified Jelly Roll (MJR), Internal Tin (low-tin ITER type), and Powder-in-Tube (PIT) technologies

Manuscript received September 17, 2000. This work was supported by the US Department of Energy.

E. Barzi, M. Fratini, R. Yamada, and A. V. Zlobin are with Fermilab, MS 316, Batavia, IL 60510 USA (telephone: 630-840-3446, e-mail: [barzi@fnal.gov](mailto:barzi@fnal.gov)).

R. M. Scanlan and H. C. Higley are with Lawrence Berkeley National Laboratory, Berkeley, CA 94720.

TABLE I  
STRAND PARAMETERS

Strand Parameter	OST	IGC (ITER)	SMI
Strand diameter, mm	1.000±0.003	1.000±0.003	1.005±0.003
J <sub>c</sub> (12T), A/mm <sup>2</sup>	> 1900	>700	> 2100
I <sub>c</sub> (12T), A	> 800	>200	> 900
d <sub>eff</sub> , μm	< 110	<5	< 50
Cu, %	48 ± 0.3	58.7± 0.3	45.3 ± 0.3
RRR	< 20	>300	> 100
Twist pitch, mm/turn	25 ± 10	13± 3	20 ± 3

were purchased by Fermilab from Oxford Superconducting Technology (OST), Intermagnetics General Corporation (IGC), and Shape Metal Innovation (SMI) respectively [3]. The OST, IGC (ITER) and SMI strand parameters are shown in Table I.

Short samples of 28 strand cables with rectangular and keystone cross-section, and different packing factor were fabricated with and without a stainless steel core, using a constant transposition pitch of 109.8 mm. The cable packing factor, *PF*, is defined as the ratio of the cross section occupied by the strands to the overall cross section of the cable:

$$PF = \frac{n\pi d^2}{4(wt - A_{Core}) \cos \psi}, \quad (1)$$

where *n* is the number of strands in the cable, *d* is the strand diameter, *w* and *t* are the average width and thickness, *ψ* is the lay angle, and *A<sub>Core</sub>* the cross sectional area of the core.

The different packing factors were obtained by varying cable mean thickness, whereas cable width, lay angle, and the keystone angle, *α*, were kept within 14.24±0.025 mm, 14.5±0.1 degree, and 0.9±0.1 degree respectively. For rectangular cables, *α* was 0.0±0.1 degree. Tables II, III and IV show the cable parameters.

TABLE II  
SMI CABLE PARAMETERS

Cable No.	Core <sup>a</sup>	Type <sup>b</sup>	Thickness, mm	<i>PF</i> , %
1	Y	KS	1.842	88.3
2	Y	KS	1.817	89.6
3	Y	KS	1.787	91.1
4	Y	KS	1.764	92.4
5	Y	KS	1.736	93.8
6	Y	R	1.911	84.7
7	Y	R	1.851	87.8

<sup>a</sup> Stainless steel core, 9.525mm x 0.025mm, 316-L annealed.

<sup>b</sup> R = Rectangular cable, KS = Keystoned cable.

TABLE III  
OST CABLE PARAMETERS

Cable No.	Core <sup>a</sup>	Type <sup>b</sup>	Thickness, mm	PF, %	HT No.
745-B	N	R	1.885	84.4	3
745-C	N	R	1.839	86.6	3
745-D	Y	R	1.881	85.8	2
745-F	Y	R	1.842	87.6	1
746-A	N	KS	1.828	87.3	1
746-D	N	KS	1.774	90.0	1
746-E	N	KS	1.750	91.3	3, 4
746-F	N	KS	1.690	94.5	1
746-H	Y	KS	1.823	88.7	3, 4
746-I	Y	KS	1.808	89.4	2
746-J	Y	KS	1.759	92.0	2
749	Y	KS	1.750	92.3	2
746-K	Y	KS	1.730	93.6	2
746-G	Y	KS	1.706	94.9	2

<sup>a</sup> Stainless steel core, 12.7mm x 0.025mm, 316-L annealed.

<sup>b</sup> R = Rectangular cable, KS = Keystone cable.

TABLE IV  
IGC (ITER) CABLE PARAMETERS

Cable No.	Core <sup>a</sup>	Type <sup>b</sup>	Thickness, mm	PF, %
1	N	R	1.876	84.9
2	Y	R	1.848	87.6
3	N	KS	1.850	86.1
4	N	KS	1.799	88.7
5	N	KS	1.795	88.9
6	N	KS	1.761	90.7
7	N	KS	1.715	93.2
8	Y	KS	1.909	84.5
9	Y	KS	1.835	88.1
10	Y	KS	1.800	89.8
11	Y	KS	1.780	90.9
12	Y	KS	1.756	92.2

<sup>a</sup> Stainless steel core, 12.7mm x 0.025mm, 316-L annealed.

<sup>b</sup> R = Rectangular cable, KS = Keystone cable.

### B. Strand Preparation and Measurement Procedure

For this study, four sets of OST samples, one set of IGC (ITER) and one set SMI samples were used. Each set included virgin (round) strands and strands extracted from the cables. These sets were heat treated in argon atmosphere according to the schedules given in Table V.

TABLE V  
HEAT TREATMENT SCHEDULES

Cable	Heat treatment <sup>a</sup>	Step 1	Step 2	Step 3
OST	HT-1	Temperature, °C	575	700
		Duration, h	200	30
	HT-2	Temperature, °C	575	700
		Duration, h	200	40
HT-3	Temperature, °C	575	700	
	Duration, h	200	50	
HT-4	Temperature, °C	210	575	700
	Duration, h	100	200	30
IGC (ITER)	HT-5	Temperature, °C	575	700
		Duration, h	200	80
SMI	SMI	Ramp rate, °C/h	150	120
		Temperature, °C	590	675
		Duration, h	1/3	62

<sup>a</sup> Unless otherwise specified, the temperature ramp rate is 25°C/h.

A different thermal cycle was used for each set of OST samples to monitor the dependence of  $I_c$  degradation on heat treatment (HT). Table III specifies the HT number of each OST sample.

Voltage-current (VI) characteristics were measured in boiling He at 4.2 K, in a transverse magnetic field, B, from 11 T to 15 T. The voltage was measured along the sample by voltage taps placed 50 cm apart. The sample critical current  $I_c$  was determined from the VI curve using the  $10^{-14} \Omega\cdot m$  resistivity criterion. The relative directions of magnetic field and transport current generate an inward Lorentz force. The differential thermal contraction between sample and barrel produces a tensile strain of 0.11% on the specimen. By including the Lorentz force contribution, the total tensile strain on the sample is 0.05% at 12 T and 4.2 K. This leads to a positive shift of 3-5% on  $I_c$  [4]. The n-values were determined from the VI curve in the voltage range from  $V(I_c)$  to  $10 \cdot V(I_c)$  using the power law  $V \sim I^n$ . The estimated uncertainty of the  $I_c$  measurements in this study is within  $\pm 1\%$  at 4.2 K and 12 T, and it is about  $\pm 5\%$  for the n-values.

## III. TEST RESULTS AND DISCUSSION

### A. $I_c$ Measurements of Virgin and Extracted Strands

The results of critical current measurement for virgin and extracted strands are shown in Fig.1 as a function of magnetic field for two representative samples (maximum and minimum packing factor PF) of OST, IGC (ITER) and SMI cored cables. For the same samples, the  $I_c$  degradation, expressed as the  $I_c$  of an extracted strand normalized to the  $I_c$  of the virgin strand, is shown in Fig.2 as a function of B. As can be seen, the  $I_c$  degradation is sensitive to magnetic field.

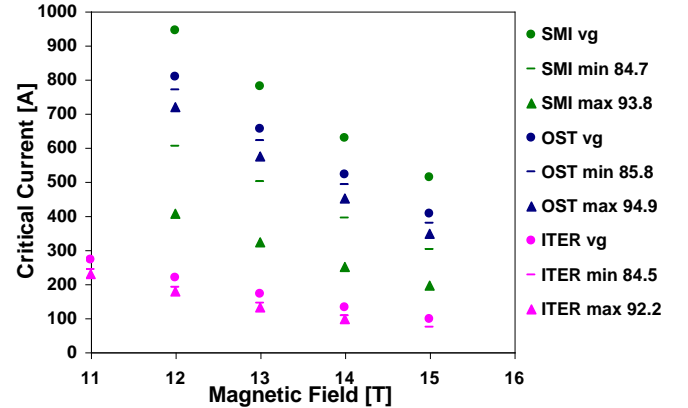


Fig. 1. Dependence of  $I_c$  on field for virgin and extracted strands of two representative samples (maximum and minimum PF) of OST, SMI and ITER cored cables.

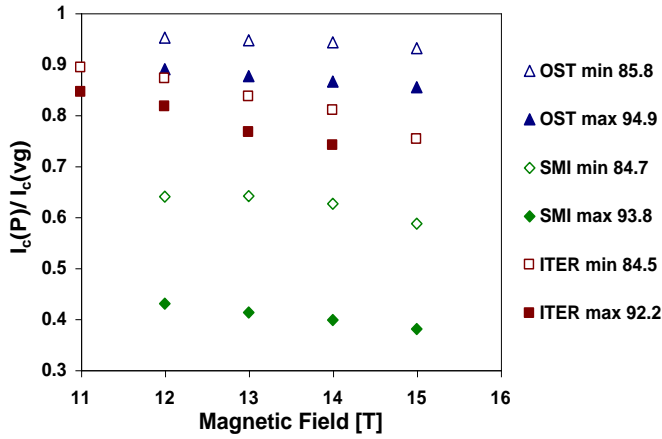


Fig. 2. Normalized  $I_c$  as a function of magnetic field for representative (maximum and minimum  $PF$ ) extracted strands.

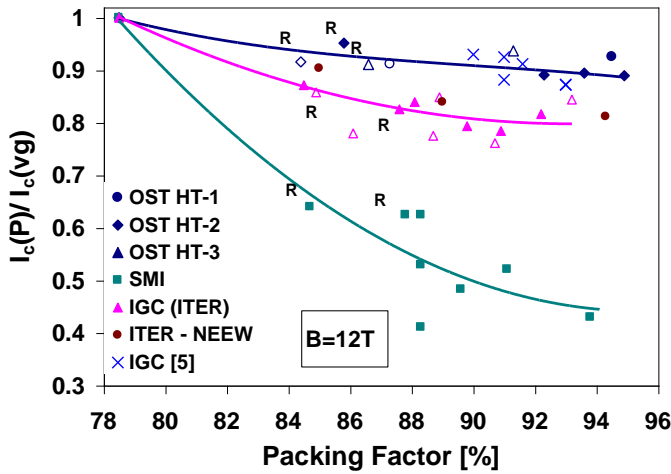


Fig. 3. Effect of  $PF$  on  $I_c$  degradation at 12 T for all cables. Rectangular cables are marked  $R$ . Unfilled markers stand for cables without the core.

The  $I_c$  degradation of all tested cables as a function of  $PF$  is shown at 12 T in Fig. 3. A normalized  $I_c/I_c(vg)=1$  is assigned to  $PF=78.5\%$ , which is the value of an undeformed round strand inscribed in a square. Not all samples produced results at 12 T due to quenching. At 15 T the figures presented very similar trends, albeit with a higher degradation.

The above results show that for all three  $Nb_3Sn$  technologies the  $I_c$  degradation due to cabling increases with increasing  $PF$ . These data do not indicate a dependence on there being a core in the cable, nor on the cable being keystone or rectangular.

The  $I_c$  degradation is relatively low for the cables made of MJR strands. For the cable with the largest packing factor of 94.9% the  $I_c$  degradation is 11% at 12 T and less than 15% at 15 T. No effect related to heat treatment could be determined even at high fields, where more data were available. This is consistent with [5].

The IGC low tin strand developed for ITER appears to behave differently from the more recent Internal Tin IGC technology [5]. At 12 T, the average degradation for the IGC ITER strand was 18% (rms=4%), whereas higher tin IGC

strands had an average degradation of 10% (rms=3%)[5].

The PIT strands present the largest degradation among all tested strands. The cable with the smallest packing factor of 84.7% produces an  $I_c$  degradation as high as 36% at 12 T.

### B. Discussion

In order to understand possible causes of  $I_c$  degradation after cabling, additional studies were performed.

Fig. 4 shows the degradation of  $n$ -value at 12T of all tested cables as a function of  $PF$ . The  $n$ -value is a quality factor related to the longitudinal uniformity of the superconducting filaments. For the OST strands, the degradation in  $n$ -value ranges from 5 to 35%, whereas the  $n$ -value reduction of the SMI is greater than 70% for all packing factors. This shows great damage in the filaments. The data obtained on IGC ITER strands give an indication that a core may help to reduce  $n$ -value degradation. The average  $n$ -value reduction was 34% (rms=7%) in the presence of a core, and 43% (rms=6%) without.

Damage of the diffusion barrier and tin leakage into the outer copper were also studied by measuring the copper residual resistivity ratio (RRR) and by analyzing strand cross-sections before and after cabling.

The measured values of RRR (at zero magnetic field) of all extracted strands as a function of  $PF$  are shown in Fig. 5. The RRR data for OST and IGC (ITER) strands show no significant effect due to packing factor. The original high RRR of about 200 of the IGC (ITER) virgin strand is maintained after cabling, as is the lower RRR (20 to 60) of the OST round strand. In the former case, the Ta barrier withstands both the thermal cycle and the cabling process, whereas in the latter case, the Nb barriers cede and leak Sn in the surrounding Cu stabilizer already during heat treatment of a virgin round wire. It is clear that this picture does not improve with cabling. On the other hand, for the SMI strand Sn contamination is not independent from cabling. At its minimum packing factor, the SMI RRR has already fallen to half its value. It is apparent that in this case a great damage has been done to the Nb filaments, consistently with the  $n$ -value results.

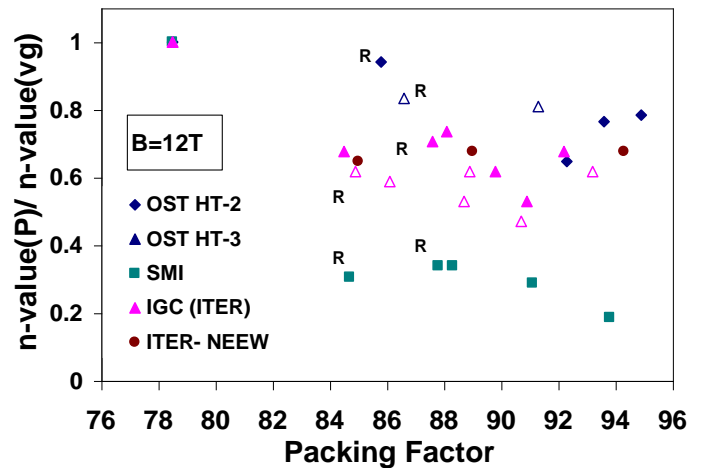


Fig. 4. Effect of  $PF$  on  $n$ -value degradation at 12 T for all cables. Rectangular cables are marked  $R$ . Unfilled markers stand for cables without

the core.

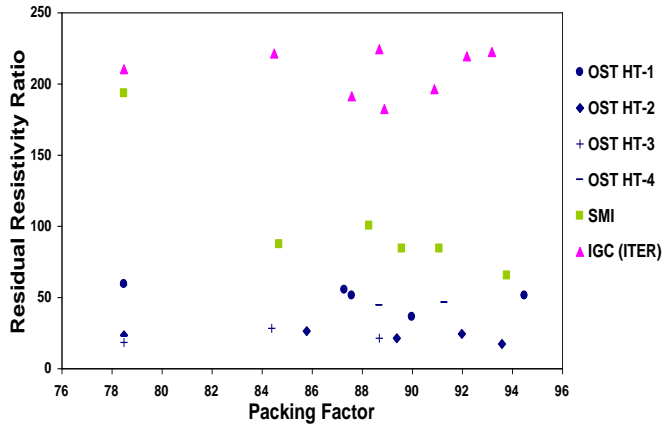


Fig.5. Effect of PF on RRR for all cables.

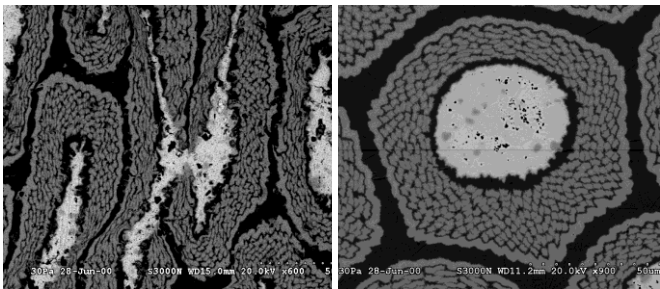


Fig.6. SEM pictures of a damaged zone in cable OST 746-I (left) and undeformed OST subelement (right).

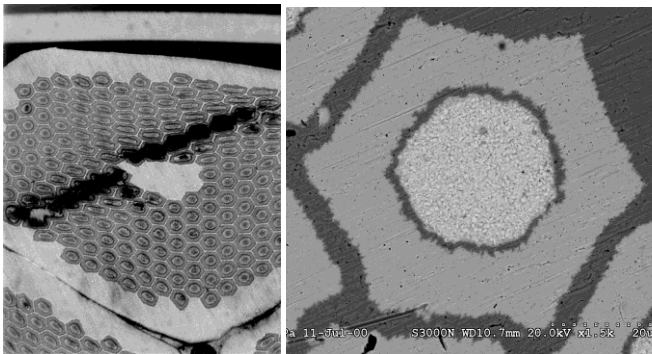


Fig.7. Left: damage in keystone PIT cable #1 (Courtesy Kelly Molnar, LBNL). Right: undeformed SMI filament.

These conclusions were confirmed by the images presented in Figs. 6 and 7. As can be seen, severe deformation and damage of the internal structure of the strands occurred after cabling. For the MJR strand, this includes breakage of the diffusion barrier and subelements intermixing, for the PIT strand, dislocation and mechanical separation of the filaments. This is very likely to affect the strand  $I_c$  degradation. It is remarkable that the mechanical damage in the MJR strand did not result in large  $I_c$  and  $n$ -value degradation, but only in a reduction of the RRR. However, in the PIT strand the mechanical damages were most likely the main cause of  $I_c$  degradation.

#### IV. SUMMARY

Studies of cable  $I_c$  degradation and its dependence on the strand packing factor have been performed for  $Nb_3Sn$  strands fabricated with various technologies (IT, MJR and PIT). Using the same cable design has allowed distinguishing the effect for different strands. The  $I_c$  degradation varies from 10 to 60%. The maximum value was observed for the PIT strand. Degradation of  $n$ -value, and matrix contamination in the extracted strands were also observed. The analysis of strand cross sections before and after cabling showed large structural damages in both OST and PIT strands. For the PIT strand, these damages were crucial, whereas they did not so much degrade the  $I_c$  performance of the OST strand. The results obtained demonstrate that the  $I_c$  degradation due to plastic deformations occurring during cabling is an important parameter to be taken into account in  $Nb_3Sn$  strand R&D.

#### ACKNOWLEDGMENT

The authors thank Jay A. Hoffman for his infinite patience in preparing the molds for microscopy for this and for many other works.

#### REFERENCES

- [1] G. Ambrosio et al., "Development of the 11T  $Nb_3Sn$  dipole model at Fermilab", IEEE Transactions on Applied Superconductivity, v. 10, No. 1, March 2000, p.298.
- [2] L. F. Goodrich et al., "Superconductor critical current standards for fusion applications", NISTIR 5027, NIST.
- [3] E. Barzi et al., "Study of  $Nb_3Sn$  strands for Fermilab's high field dipole models", this Conference.
- [4] E. Barzi et al., "Error analysis of short sample  $J_c$  measurements at the Short Sample Test Facility", Fermilab, TD-98-055, September 1998.
- [5] E. Barzi et al., "Study of strand critical current degradation in a Rutherford type  $Nb_3Sn$  cable", CEC/ICMC'99, Montreal, Canada, July 12-17, 1999.